Title

In situ formed polymer gel electrolytes for lithium batteries with inherent thermal shutdown safety features

Journal

Journal of Materials Chemistry A, 7(28)

ISSN

2050-7488

Authors

Zhou, Hongyao
Liu, Haodong
Li, Yejing
et al.

Publication Date

2019-07-16

DOI

10.1039/c9ta02341k

Peer reviewed

Journal of
Materials Chemistry A

Materials for energy and sustainability

Accepted Manuscript

This article can be cited before page numbers have been issued, to do this please use: H. Zhou, H. Liu, Y. Li, X. Yue, X. Wang, M. Gonzalez, Y. S. Meng and P. liu, *J. Mater. Chem. A*, 2019, DOI: 10.1039/C9TA02341K.

ROYAL SOCIETY OF CHEMISTRY

rsc.li/materials-a

View Article Online
DOI: 10.1039/C9TA02341K

ARTICLE

In-situ formed polymer gel electrolytes for lithium batteries with inherent thermal shutdown safety features

Received 00th January 20xx,
Accepted 00th January 20xx

DOI: 10.1039/x0xx00000x

Hongyao Zhou,† Haodong Liu,† Yejing Li, Xiujun Yue, Xuefeng Wang, Matthew Gonzalez, Ying Shirley Meng and Ping Liu*

Rechargeable lithium metal batteries based on organic electrolytes face challenges in both lithium metal cycling stability and associated safety issues. Herein, we demonstrate an in-situ formed polymer gel electrolyte which enables dendrite-free lithium metal cycling. Moreover, the gel electrolyte goes through further polymerization at elevated temperatures and loses its ionic conductivity, effectively shutting down the battery. When lithium iodide (LiI) is dissolved in vinylene carbonate (VC), LiI induces the polymerization of VC to form poly(vinylene carbonate) (polyVC). The electrolyte then transforms into a polymer gel electrolyte with VC plasticizing polyVC, and with LiI as the salt. At room temperature, the gel electrolyte enables dendrite-free lithium metal cycling at current densities as high as 5 mA cm^{-2} for 500 cycles. Further, a Li/ $Li_4Ti_5O_{12}$ (LTO) cell retains 50% of the initial capacity at the 700th cycle. When the cell is heated to 80 °C, the ionic resistance of the electrolyte increases by a factor of 10^3, resulting in a shutdown of the cell due to the complete polymerization of VCs. The approach of using in-situ polymerization to enable stable lithium cycling as well as to serve as thermally triggered shutdown mechanism provides a new pathway of making safer lithium metal batteries.

Introduction

Rechargeable lithium (Li) metal batteries are being intensively studied due to their promises of high energy densities.[1] Current research focuses on addressing the cycle life issues of the Li metal anode.[2–4] Li metal is known to experience dendrite growth. Coupled with its high reactivity with the organic electrolyte, continuous consumption of electrolyte and the formation of isolated "dead" lithium leads to cell failure.[5] Another challenge of Li metal battery is an increased concern for safety. Flammability of organic solvent is an inherent safety problem of using liquid-based electrolytes including polymer gel electrolytes.[6] The safety issue is more pronounced in Li metal battery, where highly reactive, mossy Li metal grown on the anode is prone to catch fire.

Current research on Li metal anode overwhelmingly focuses on improving its cycling stability by suppressing dendrite (or more generally non-uniform) growth and improving coulombic efficiency. General approaches include: 1) three-dimensional (3D) hosts to minimize macroscopic volume change and reduce local effective current density which discourages dendrite growth;[7,8] 2) new electrolyte chemistry to affect Li deposition.[9,10] For example, ether-based electrolyte was found to be more effective than carbonate-based electrolytes to offer dendrite-free Li deposition;[11,12] and 3) inorganic and polymeric coatings to influence morphology.[13–15]

The fundamental reason for non-uniform Li growth is due to uneven current distribution, ion concentration gradient in the solution and the heterogeneous nature of the Li surface especially at a high current density. Li chemically reacts with electrolyte components (both solvent and salts) to form the solid electrolyte interface (SEI) layer, which is a composite of multiple salts and organic and polymeric compounds.[16] The heterogeneous nature of the SEI layer inherently leads to inhomogeneous Li metal growth. Based on this hypothesis, we previously fabricated a single component layer of lithium methyl carbonate (LMC) on the surface of Li metal by reacting dimethyl carbonate (DMC) and lithium iodide (LiI) and achieved a stable plating/striping of Li in a mixed electrolyte of ethylene carbonate (EC), DMC and LiI.[17,18] LiI works as both a source of lithium ion and a catalyst of the demethylation of DMC, which produces LMC. This rigid inorganic layer on Li metal is chemically homogeneous and suppresses the dendrite growth.

Compared to tremendous efforts to increase the lithium cycling stability and efficiency, much less attention has been paid to the safety implications of electrolyte choices. Although ether based solvents are favored for high-efficiency lithium cycling, they are highly volatile. Recently, researchers proposed to use electrolytes with very high concentrations of salts to achieve simultaneous excellent cycle life and safety in both lithium-ion and Li metal batteries. Yamada et al. showed high concentration of lithium/sodium bis(fluorosulfonyl)imide (LiFSI/NaFSI) in TMP (trimethyl phosphate) solvent exhibits both fire retarding property and highly reversible cycling of Li^+ or Na^+ ions with graphite anodes.[19] Zhang et al. reported that the

[a] Department of NanoEngineering, University of California San Diego, 9500 Gilman Drive, La Jolla, CA 92093, United States

†These authors contributed equally to this work.

Electronic Supplementary Information (ESI) available. Results of GC-FID experiment; reaction schemes of the polymerization; fabrication of the gel Li metal cell; Li deposition under no external pressure; preparation of LTO cathode. See DOI: 10.1039/x0xx00000x

View Article Online
DOI: 10.1039/C9TA02341K

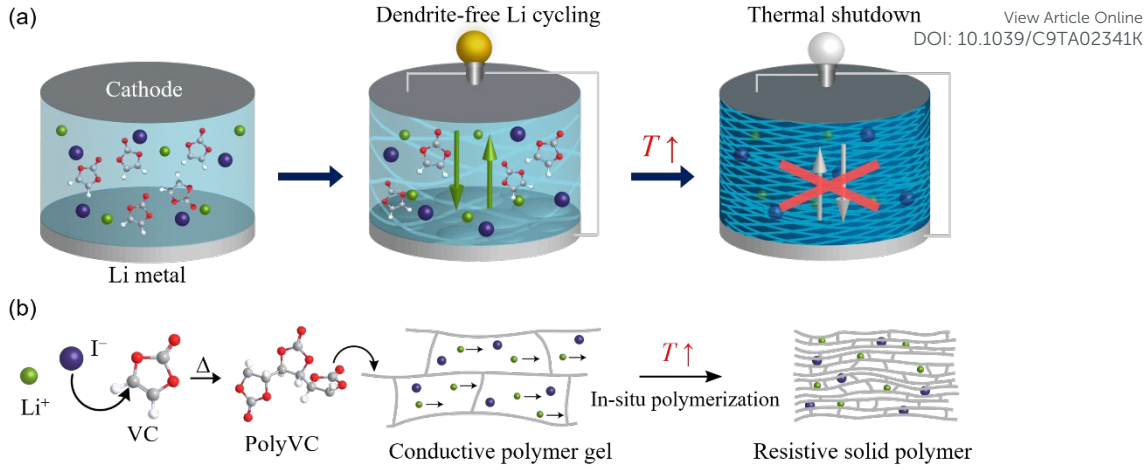

Figure 1. (a) Li metal battery enabling dendrite-free Li cycling at room temperature and thermal shutdown when temperatures increase. (b) Chemical reactions and physical state of the polyVC-LiI gel inside the battery represented in (a). Heating of the electrolyte within a controlled time triggers partial polymerizations of VC with I^- anion to form the polymer gel network. Prolonged time of heating leads to full polymerization of VC and results in the resistive solid phase.

highly concentrated LiFSI in triethyl phosphate (TEP) solution can be diluted with fluoroether, a non-solvating solvent, to decrease the total concentration of the salt, while maintaining the fire retarding property and enabling the cycle of Li metal anode at high columbic efficiency (>99%).[20]

Here, we present a new electrolyte for Li metal batteries that enables both stable lithium cycling and a new built-in safety mechanism that is thermally triggered. A polymer gel electrolyte is in-situ formed between the solvent, VC, and the salt, LiI. Contrasted from our previous work on the rigid DMC coating, the product from VC and LiI is a flexible polymer gel, which is more capable of accommodating the volume change of the Li metal anode. The SEI layer between the gel electrolyte and Li metal is composed of soft polyVC embedded with hard Li_2CO_3 nanoparticles, which enables stable Li metal cycling. The coulombic efficiency of Li plating/stripping on Cu substrate is evaluated as 98.6%. As a safety function, the gel electrolyte can solidify at elevated temperatures, lose its ionic conductivity, and shut down the battery.

Experimental

Preparation of polyVC-LiI gel electrolyte. 0.268 g of LiI (Ultra dry, >99%, Alfa Aesar, U.S.) and 2.0 g of VC (BASF, U.S.) were mixed in a 20 mL glass vial, and the solution was stirred by a magnetic stirrer at 350 rpm and heated by a hotplate at 80 °C for 1 hour. The cap of the vial should be slightly open to allow the pressure release, because the reaction between VC and LiI generates CO_2 gas. All synthesis was conducted inside an Ar-filled glove box. Free-radical polymerization of VC by AIBN was carried out based on the method reported by Reimschuessel and Creasy.[21] Anionic polymerization of VC by LiOEt was carried out in DMSO at 80 °C with monomer/initiator ratio of 100 : 1. Synthesized polymer was purified in deionized water and dried under vacuum.

Characterization. As-prepared polyVC-LiI gel was purified by a dilution in *N*,*N*-dimethylformamide (DMF, Fisher Scientific, U.S.) followed by a precipitation in methanol and rinsing with deionized water. The sample was dried under vacuum at 100 °C for 4 days. The molecular structure of the dried sample was analyzed with ATR-FTIR (UATR 2, PerkinElmar, U.S.), and 500 MHz NMR (ECA 500, JEOL, Japan). Deuterated dimethylsulfoxide (d_6-DMSO, Sigma Aldrich, U.S.) was used as the solvent in the NMR experiment. The crystal structure of polyVC-LiI electrolyte after the complete polymerization was analyzed with XRD (D2 Phaser, Bruker, Germany).

The cross-sectional image and the surface morphology of polyVC-LiI gel electrolyte on Li metal/Cu foil was characterized by SEM (FEI Quanta FEG 250, Thermo Fisher Scientific, U.S.), paired with EDX analysis of C Kα, O Kα and I Lα lines with an electron beam of 10 keV. Cryo-EM micrographs were recorded on a field emission gun JEM-2100F (JEOL), equipped with an OneView camera and operated at 200 keV.[18] The pristine polyVC-LiI gel electrolyte was diluted by 10 times in VC and casted on a TEM grid. The electrodeposited Li metal was dispersed in VC under sonication and dropped on a TEM grid. All the sample preparation and transformation were performed with Ar protection.[22] The images were taken after the temperature was equilibrated to 100 K.

Electrochemical tests. The surface of Li metal was cleaned by scrubbing with a plastic blade before use. As-prepared polyVC-LiI gel was soon transferred between two pieces of Li metal and sealed in a CR2016 stainless steel coin cell case for Li//Li symmetric cell.

A copper (Cu) foil which was cleaned with hydrochloric acid was used in Li//Cu cell for the efficiency test. Prior to the test, a conditioning cycle was carried out on all the cells. In this step, a Li film was first deposited onto the Cu foil at 0.5 mA cm^{-2} for 10 hours, and then fully stripped to 1 V. Another Li film (5 mAh cm^{-2}) was deposited again, only 1 mAh cm^{-2} capacity of Li film was stripped and plated for 10 cycles. Finally, the Li film was fully stripped to 1 V. The current density during this test was 0.5 mA cm^{-2}. The distance between the two electrodes was controlled by a polypropylene film (25 µm) or a PTFE washer (125 µm) in the middle. The active diameter of the electrode is 12 mm (ESI). Electrochemical test was carried out on LAND-CT2001 battery

View Article Online
DOI: 10.1039/C9TA02341K

testing systems (LAND electronics, China) and Arbin-BT2000 battery tester (Arbin Instrument, U.S.).

Conductivity of the polymer gel was measured with a potentiostat VSP-300 (Biologic Instrument, U.S.). The gel was placed between two stainless steel rods (diameter = 6.35 mm, distance = 3.0 mm) and heated with ribbon heater. Alternating voltage (10 mV) was applied after the temperature was stabilized (dT/dt < 0.1 °C min^{-1}).

Electrochemical window of the polymer gel electrolyte was evaluated with cyclic voltammetry, using a three electrode cell: the working electrode was a stainless steel foil (SUS304, area = 0.7 cm^2); the reference and the counter electrodes were Li metal foil. The voltage range was between –0.15 and 3.8 V vs. Li/Li$^+$, and the scan rate was 1 mV s^{-1}.

Results and discussion

Formation and mechanism of thermal shutdown of polyVC-LiI gel electrolyte. A polymer gel electrolyte is synthesized by the gelation of a solution of VC and LiI (1 mol kg^{-1}) with a controlled reaction time (1 h) at 80 °C. LiI is the catalyst for the polymerization of VC. The polymerization rate significantly reduces at room temperature, especially when the polymer gel electrolyte is sealed in a battery cell. The reduction of VC on the surface of Li metal forms a robust SEI layer and enables dendrite-free cycling of the Li metal battery (**Figure 1**a). When the battery is heated, the polymerization of VC is accelerated, and the gel electrolyte turns into a solid phase (Figure 1b). Low ionic conductivity of the solidified electrolyte hinders the Li$^+$ ion transport and stops the charging/discharging of the battery.

Molecular structure of polyVC and the polymerization mechanism of VC catalyzed by LiI. The polymer gel synthesized with LiI was black in color (Figure S1, ESI). Weight ratio of the polymer to VC solvent in the gel is 20% as determined by precipitating the polymer fraction in methanol from a DMF solution. The molecular weight of the polymer shows broad distribution ranging from 10^3 to 10^5 Da, as analyzed by gel permeation chromatography (Figure S1c, d ESI). VC was also polymerized by free-radical and anionic polymerizations with azobisisobutyronitrile (AIBN) and lithium ethoxide (LiOEt) as initiators, respectively, to compare with the molecular structures of polyVC initiated from LiI. Despite the fact that free-radical polymerization of VC by AIBN has been studied for decades,[21,23,24] to the best of our knowledge, there are no reported studies on anionic polymerization of VC. The polymer products were precipitated in water and dried at 100 °C under vacuum overnight. Fourier-transform infrared (FTIR) spectra of three types of polyVCs prepared by AIBN, LiOEt, and LiI are shown in **Figure 2**a. The C-H alkane stretching at 2990 cm^{-1} in those three polyVCs derives from the addition reaction on the double bond of VC. The C=O carbonyl stretching (1800 cm^{-1}) and C-O-C carbonate ester stretching (1160 & 1080 cm^{-1}) are present in those three polyVCs, which indicates the cyclic carbonate unit is preserved after the polymerization.

An additional peak at 970 cm^{-1} is particularly pronounced in polyVCs initiated by LiI and LiOEt. The five-membered ring of VC is not stable on the anionic attack from alkoxide or I$^-$, and ring-opening reaction can take place. Production of CO_2 gas from the solution of VC and LiI is observed by gas chromatography with a flame ionization detector (GC-FID) (Figure S2, ESI). The rate of CO_2 gas generation increases at a higher temperature. Krapcho reported that nucleophilic attack from anions can promote the decarboxylation of the substrate in a concerted fashion.[25] The IR peak at 970 cm^{-1} is assigned to C-O-C ether stretching, resulting from the ring-opening and decarboxylation reaction of the cyclic ester bond. Indeed, anionic polymerization of ethylene carbonate (five-membered cyclic carbonate) also produces ring-opened structure.[26,27]

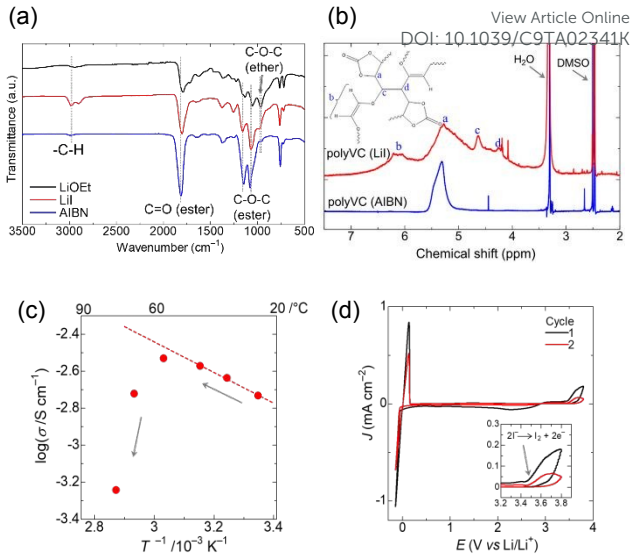

Figure 2 (a) IR spectra of polyVCs polymerized with AIBN, LiI, and LiOEt as the initiator. (b) ^{1}H NMR spectra of polyVCs polymerized with AIBN and LiI. (c) Conductivity of polyVC-LiI electrolyte at increasing temperature (average heating rate is 0.3 °C min^{-1}). (d) Cyclic voltammetry of the polyVC-LiI electrolyte on a stainless steel working electrode. Scan rate was 1 mV s^{-1}.

^{1}H NMR analysis (Figure 2b) confirms polyVC initiated by AIBN has the simplest molecular structure, only possessing the cyclic carbonate units (peak **a**, chemical shift: 5.3 ppm). The main peak of polyVC initiated by LiI matches with peak **a** and two additional peaks (**b**, **c**) are present. A broad peak (**b**) between 6.0 and 6.2 ppm is assigned to H on vinyl group and peak **c** at 4.6 ppm to H on tertiary carbon bonded with oxygen atom and ethylene carbonate unit. The presence of vinyl group supports the ring-opening reaction during the polymerization, and tertiary carbon suggests a branched structure in the cyclic carbonate chain.

According to our observation that the polymerization of VC proceeds with the decarboxylation, lithium iodoalkoxide (by-product of the decarboxylation of VC) is likely the initiator of the polymerization (see Figure S3 in the ESI for the reaction scheme). Alkoxide attacks the double bond of VC and the polymerization propagates. Substitution reaction of iodo group by alkoxide adds vinyl ether group in the polymer structure and regenerates the I$^-$ anion. Ring-opening reaction can occur on the main chain of cyclic carbonate in polyVC. Branching of the polymer chain is then accomplished by the substitution reaction of iodo group by anionic end group of another polymer chain.

A solution of VC and LiI (1 mol kg^{-1}) was stored at room temperature under Ar atmosphere for a prolonged period time

View Article Online
DOI: 10.1039/C9TA02744K

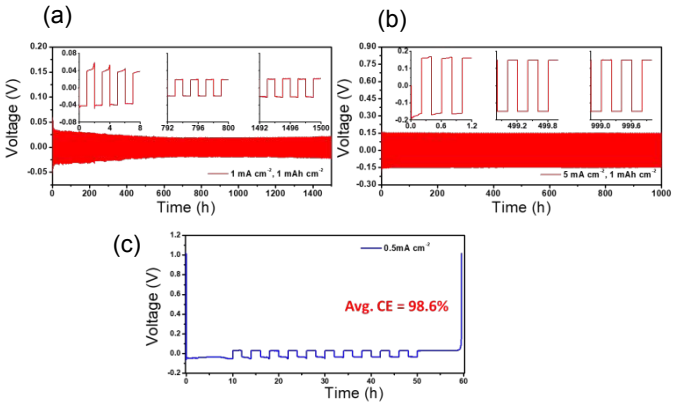

Figure 3. Cycling performance of Li//Li symmetric cell with separator-free polyVC-LiI gel electrolyte at a current density of (a) 1 mA cm^{-2} and (b) 5 mA cm^{-2}. (c) Efficiency test of Li plating/stripping with Li//Cu cell. Thickness of the gel electrolyte is: (a) 25 μm; (b, c) 125 μm.

to study the composition and the crystal structure. The sample gradually turned to a gel and finally to a hard solid after five months. IR spectra of the solid polyVC-LiI electrolyte only shows the peaks of polyVC and unreacted residual VC (Figure S4a, ESI). The catalytic reaction between LiI and VC is specific, and polyVC and CO_2 are the only major products. Interestingly, powder X-ray diffraction (PXRD) of the polyVC-LiI electrolyte shows only a broad peak of polyVC, and LiI is completely amorphized in the polymer matrix (Figure S4b, ESI).

Conductivity and electrochemical window of polyVC-LiI gel electrolyte. The conductivity of the polyVC-LiI gel electrolyte at 25 °C is evaluated as 1.8×10^{-3} S cm^{-2}, which is comparable to the conductivities of other organic liquid electrolytes. The conductivity increases linearly with increasing temperatures (average heating rate was 0.3 °C min^{-1}) until 60 °C, following the Arrhenius equation (Figure 2c). However, the conductivity starts decreasing above 60 °C, because polymerization of VC solidifies the electrolyte. Decay of the conductivity at high temperatures is expected to shut down the battery.

The electrochemical window of the polyVC-LiI gel electrolyte was analyzed by cyclic voltammetry (Figure 2d). The electrolyte was very stable down to lithium plating potential but oxidative current was observed above 3.5 V vs. Li/Li$^+$, which is due to the oxidation of iodide anion in the electrolyte. The oxidation potential of LiI in the polyVC-LiI gel electrolyte is higher than the oxidation potential in a liquid ether electrolyte (2.9 V vs. Li/Li+).[28]

Electrochemical performance of Li metal anode with polyVC-LiI gel electrolyte. The polyVC-LiI gel was directly applied as the electrolyte in Li//Li symmetric cell. In order to examine the intrinsic property of this gel electrolyte, a plastic washer was used to control the thickness of the electrolyte instead of using a membrane support (Figure S5, ESI). With the electrolyte thickness of 25 μm, Li/polyVC-LiI/Li cell can cycle over 1500 hours without shorting at a constant current density of 1 mA cm^{-2} and areal capacity of 1 mAh cm^{-2} (**Figure 3**a). With a thicker electrolyte (125 μm), the cell can be cycled at a higher current density of 5 mA cm^{-2} (Figure 3b). The polarization in the voltage curve becomes flat after a couple of cycles at the beginning, which indicates stable plating and dissolution of Li metals.[29] Coulombic efficiency of lithium deposition in this polyVC-LiI gel was evaluated by plating/stripping Li metal on Cu foil (Figure 3c), and a high efficiency of 98.6% is achieved at 0.5 mA cm^{-2}. As a comparison, the cycling efficiency of Li metal in a carbonate electrolyte of EC/DMC/$LiPF_6$ with 2 wt% VC additive was reported as only 80%.[30] Recently, Hu and co-workers reported an electrolyte using VC as the major solvent with 1 M lithium bis(trifluoromethanesulfonyl) imide (LiTFSI) salt, and the Li cycling efficiency in this electrolyte is 97%,[31] which is comparable to the efficiency in polyVC-LiI gel electrolyte. The high efficiency of cycling Li metal suggests VC is a promising solvent to protect Li metal from parasitic side reactions with the electrolyte.

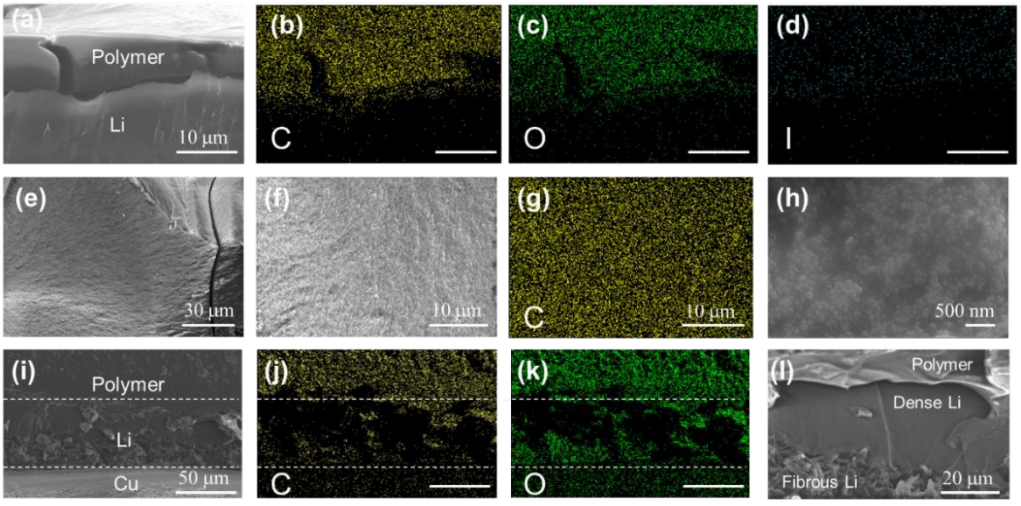

Figure 4. SEM image (a) and elemental mapping (b-d) of cross section of Li metal after cycling for 1000 hours at a current density of 5 mA cm^{-2} with a capacity of 1 mAh cm^{-2}. Scale bar = 10 μm. Surface SEM images (e, f, h) of the polymer coating on Li metal at increasing magnifications, and the elemental mapping (g) of the image (f). Cross-sectional SEM image (i) and elemental mapping (j, k) of electrodeposited Li metal on Cu substrate at a plating current density of 0.5 mA cm^{-2} with a capacity of 5 mAh cm^{-2} in polyVC-LiI gel electrolyte. Scale bar = 50 μm. (l) Magnified view of the Li metal on Cu substrate. Fibrous, and dense morphologies of Li metal are observed on the Cu side, and the polymer side, respectively.

Characterization of the interface between polyVC-LiI gel electrolyte and Li metal. The morphology of cycled Li metal and the polymer coating layer was observed by scanning electron microscope (SEM) after 1000 hours of lithium plating/stripping in a Li//Li symmetric cell at a current density of 5 mA cm^{-2} and a capacity of 1 mAh cm^{-2} (**Figure 4**a). Elemental mapping of the cross section clearly indicates the polymer layer on the lithium surface (Figure 4b-d). The surface of the polymer layer is smooth and dense (Figure 4e-h) while the cycled Li shows a dendrite-free morphology.

The morphology of Li metal deposited on Cu foil (Current density = 0.5 mA cm^{-2}, areal capacity = 5 mAh cm^{-2}) was also examined (Figure 4i-k). The dark region in the elemental mapping of C and O indicates the layer of Li metal. Interestingly, the Li metal deposited near the Cu surface shows fibrous morphology, while the Li metal is dense near the polymer electrolyte (Figure 4l). Possibly, as Li metal is deposited from the Cu substrate into the gel electrolyte the pressure on the growing tip of the Li metal increases and results in the dense morphology.

To further prove that the polymerization of VC by LiI contributes to the stabilization of Li metal, Li metal was deposited on Cu foil in VC-LiI electrolyte before and after gelation. The morphology of the electrodeposited Li metal was observed by SEM. A beaker cell was used in this experiment to eliminate the influence of pressure between the polymer gel and the electrode (Figure S6, ESI). Under the atmospheric pressure, the Li metal grows into larger particles when deposited in the gel state compared to the liquid state. To note, when $LiPF_6$ is used instead of LiI in the pure VC electrolyte, the polarization of Li plating is significantly higher and Li metal grows in a dendritic form, indicative of a beneficial role of LiI. We postulate that, unlike complex polyanions such as PF_6^-, the irreducible nature of the iodide ion prevents the formation of other inorganic anions which would introduce interfacial inhomogeneity and promote dendrite growth. The formation of the polymer gel electrolyte through selective decarboxylation and polymerization of VC thus leads to a robust and stable SEI layer consisting of Li_2CO_3 as the inorganic component and enables highly stable lithium cycling. Finally, it is also possible that high viscosity and elasticity of the gelled electrolyte enhances further the stability of the Li metal surface.[32–34]

Cryo-EM analysis of the SEI layer on Li metal. The structure and the composition of the SEI layer is directly visualized with cryogenic electron microscopy (cryo-EM) analysis.[22,35] Pristine polyVC-LiI gel electrolyte before cycling shows an amorphous structure (**Figure 5**a), and no diffraction point is observed in the fast Fourier transform (FFT) pattern in Figure 5b. This result is in agreement with the PXRD pattern of polyVC-LiI electrolyte, where LiI is completely amorphized in the polyVC matrix (Figure S4b, ESI). After 10 cycles of Li//Li cycling in polyVC-LiI gel electrolyte, Li_2O, and Li_2CO_3 particles are observed on the electroplated Li metal (Figure 5c). The FFT pattern (Figure 5d) confirms the lattice space of Li_2CO_3 (110), (200), (002) planes and Li_2O (111) plane. The Li_2O (111) plane in the marked region of Figure 5c align in the same direction, and thus those Li_2O particles likely belong to one larger particle. Li_2O comes from

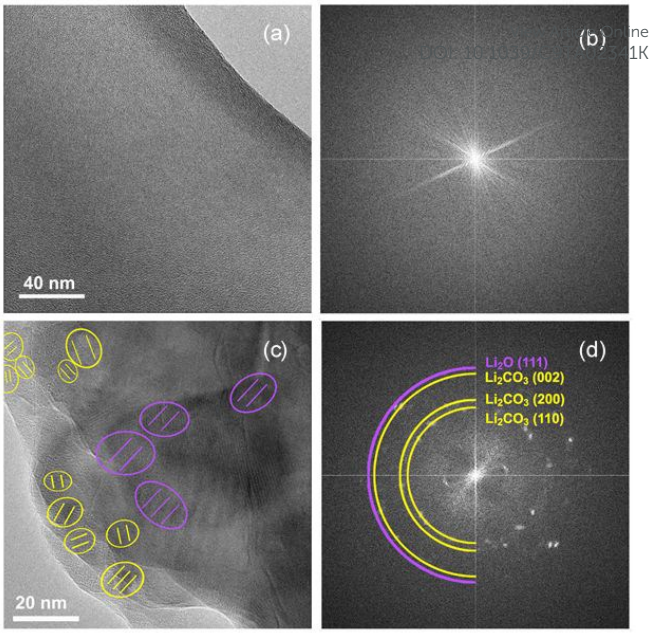

Figure 5. Cryo-EM image (a) and FFT pattern (b) of polyVC-LiI gel electrolyte. Cryo-EM image (c) and FFT pattern (d) of the SEI layer on Li metal after Li//Li symmetric cycling for 10 cycles at 1 mA cm^{-2}, 1mAh cm^{-2}. Direction of the lattice planes in each crystal grain are emphasized by the straight lines.

either surface oxidation during the sample preparation or the decomposition of VC. The particle size of Li_2CO_3 ranges from 10 to 20 nm and is larger than those (c.a. 3 nm) produced from a carbonate electrolyte of ethylene carbonate (EC)/diethylene carbonate (DEC) with 1 M $LiPF_6$.[36] The in-situ decarboxylation of VC in the electrolyte increases the concentration of CO_2 and promotes the growth of dense and large Li_2CO_3 particles. Except for Li_2CO_3 and Li_2O, no other crystalline SEI component, such as lithium methylcarbonate (LMC),[18] are observed. Amorphous region in Figure 5c is likely occupied by polyVC, as the amorphous nature is shown in Figure 5a.

We would like to put the composition and function of this unique SEI layer into the context of previous SEI engineering approaches. The chemical composition of SEIs are usually very complex, comprised of a mixture of LiF, Li_2CO_3, Li_2O, various forms of lithium alkyl carbonate, and polymers.[16,37] This is a direct result of the strong reductive ability of Li metal when exposed to organic solvents and lithium salts with complex anions. As a result, the exact role of different components in determining cycling stability is unclear. To make the case even more complex, it is a popular practice to add additives to improve the SEI. For example, fluorinated organic solvents[38–42] and fluoride salt[9,11,43] additives can preferentially be reduced at the anode, thus forming more desirable SEIs. [10,44,45] Lithium fluoride (LiF) is widely believed to be the key SEI component because of the low solubility in the electrolyte, the high electrochemical stability, and the mechanical robustness.[46] Meanwhile, the addition of CO_2 in the electrolyte is also known to improve the cycle performance, because of the formation of Li_2CO_3 in the SEI layer.[47–49]

The SEI layer made from VC and LiI in this study is free from fluoride compounds. Therefore, it is clear that Li_2CO_3 and amorphous polyVC alone are effective to stabilize the interface

View Article Online
DOI: 10.1039/C9TA02341K

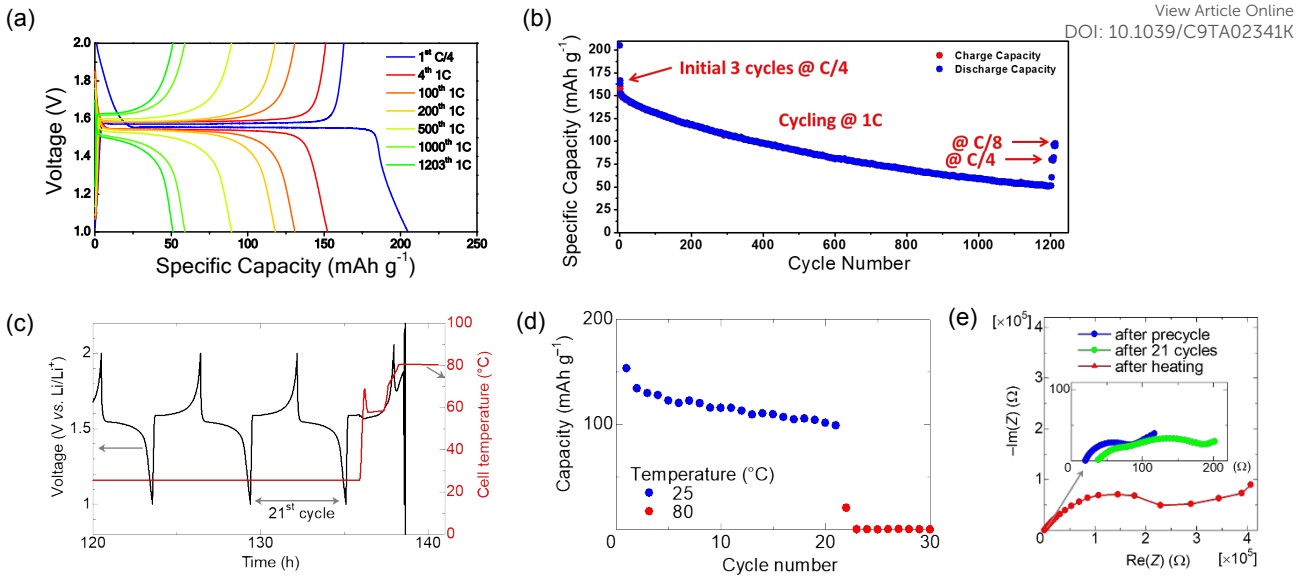

Figure 6. Voltage profile (a) and specific capacity (b) of LiI/LTO cell cycled in polyVC-LiI gel electrolyte at the indicated C-rate. (c) Voltage profile and cell temperature of Li//LTO cell. The cell temperature was increased in the middle of 22nd charging step. (d) Discharge capacity of Li//LTO cell and the cycle number. (e) Impedance spectra of Li//LTO cell after precycle (2 cycles at 20 μA cm^{-2}), 21 cycles (at 40 μA cm^{-2}), and heating at 80 °C.

between the electrolyte and Li metal. Elimination of the decomposition reaction of lithium salt by using LiI simplifies the interface chemistry and helps to define the composition of SEI layer.

Thermal shutdown of Li//LTO cell test with polyVC-LiI gel electrolyte. PolyVC-LiI gel electrolyte was tested in a full cell to demonstrate its potential application. LTO was selected as the cathode material and cycled between the cutoff voltages of 1 and 2 V vs. Li^+/Li, well below the oxidation potential of I^- (3.5 V vs. Li^+/Li). During the first discharge, an irreversible capacity of 25 mAh g^{-1} is lost in the reductive reaction of the gel electrolyte (**Figure 6a**). A passivation layer likely forms on the cathode side during this first discharge, and this irreversible reaction gradually diminishes in the following cycles. The increasing polarization with cycle numbers suggests the formation of a thicker polyVC layer on the cathode side. Since the increase of polarization was not observed in Li//Li symmetric cell during long term cycling (Figure 3a, b), polyVC-LiI gel electrolyte is more stable with Li metal compared to LTO cathode. Despite the slow capacity decay, the cell still maintains half of the initial capacity (75 mAh g^{-1}) after 700 cycles of charging/discharging at a rate of 1 C (Figure 6b). Recovery of the capacity by slowing down the charging/discharging rate (to 1/4 and 1/8 C after 1203 cycles) indicates kinetic barrier is a source of the capacity degradation.

The temperature of LTO cell was increased in the middle of the charging step at room temperatures to evaluate the thermal shutdown function. When the cell temperature is increased to 60 °C, the overpotential of the cell decreases by 20 mV, because the ionic conductivity of the electrolyte increases, while the polymerization rate is slow at this temperature (Figure 6c). When the temperature reaches 80 °C, the polymerization rate of VC is accelerated, resulting in a complete loss of the capacity within 30 min (Figure 6d). The impedance of the LTO cell increases from 200 Ω to 2×10^5 Ω after heating at 80 °C (Figure 6e), and the electrolyte turned into a solid (Figure S7, ESI). A complete polymerization of VC is triggered by the heating and successfully shuts down the cell.

Conclusions

Thermal shutdown function using a polymer gel electrolyte was demonstrated in Li metal battery for the first time. Thermally activated in-situ polymerization was successfully implemented in the self-protective battery. Combination of VC and LiI also stabilizes the surface Li metal by forming the SEI layer composed of Li_2CO_3 and polyVC. Nucleophilic attack of LiI on VC produces CO_2, and lithium alkoxide, which initiates anionic polymerization of VC. LiI is completely amorphized in the polyVC matrix. The composite SEI layer with 20 nm dense Li_2CO_3 grains embedded in amorphous polyVC matrix results in stable Li//Li symmetric cycling for over 1000 hours at 5 mA cm^{-2} and 1 mAh cm^{-2}, achieving 98.6% coulombic efficiency of Li plating/stripping. The thermal shutdown function of the gel electrolyte is also demonstrated in a Li//LTO cell with promising cycling stability. We are mindful that the use of LiI as the salt limits its upper operating voltage to 3.5 V. As a result, we are actively pursuing the use of LiI-containing polyVC gel electrolyte to enable stable cycling of sulfur-based cathodes, which will be reported elsewhere. The idea of using irreducible lithium salt (LiI) and catalyzed chemical reactions to control the composition of SEI layer leads to a better understanding of the interfacial chemistry inside batteries. The work also clearly shows the potential of a fluorine free electrolyte chemistry for Li metal batteries.

Conflicts of interest

There are no conflicts to declare.

View Article Online
DOI: 10.1039/C9TA02341K

Acknowledgements

This work was supported by the Office of Vehicle Technologies of the U.S. Department of Energy through the Advanced Battery Materials Research (BMR) Program (Battery500 Consortium) under Contract DE-EE0007764. Part of the work used the UCSD-MTI Battery Fabrication Facility and the UCSD-Arbin Battery Testing Facility. We acknowledge the UC Irvine Materials Research Institute (IMRI) for the use of the Cryo-Electron Microscopy Facility, which is funded in part by the National Science Foundation Major Research Instrumentation Program under Grant CHE-1338173. The authors are grateful to T. Kim and Prof. D. Fenning (UCSD, NanoEngineering) for the help with GC-FID measurements, Dr. D. Church and Prof. J. Pokorski (UCSD, NanoEngineering) for the help with GPC experiments.

References

1 P. Albertus, S. Babinec, S. Litzelman and A. Newman, *Nat. Energy*, 2017, **3**, 16–21.

2 X. Cheng, R. Zhang, C. Zhao and Q. Zhang, *Chem. Rev.*, 2017, **117**, 10403–10473.

3 D. Lin, Y. Liu and Y. Cui, *Nat. Nanotechnol.*, 2017, **12**, 194–206.

4 M. D. Tikekar, S. Choudhury, Z. Tu and L. A. Archer, *Nat. Energy*, 2016, **1**, 1–7.

5 D. Lv, Y. Shao, T. Lozano, W. D. Bennett, G. L. Graff, B. Polzin, J. Zhang, M. H. Engelhard, N. T. Saenz, W. A. Henderson, P. Bhattacharya, J. Liu and J. Xiao, *Adv. Energy Mater.*, 2015, **5**, 1400993.

6 S. Hess, M. Wohlfahrt-Mehrens and M. Wachtler, *J. Electrochem. Soc.*, 2015, **162**, A3084–A3097.

7 H. Liu, X. Yue, X. Xing, Q. Yan, J. Huang, V. Petrova, H. Zhou and P. Liu, *Energy Storage Mater.*, 2019, **16**, 505–511.

8 K.-H. Chen, A. J. Sanchez, E. Kazyak, A. L. Davis and N. P. Dasgupta, *Adv. Energy Mater.*, 2018, 1802534.

9 L. Yu, S. Chen, H. Lee, L. Zhang, M. H. Engelhard, Q. Li, S. Jiao, J. Liu, W. Xu and J. G. Zhang, *ACS Energy Lett.*, 2018, **3**, 2059–2067.

10 G. Li, Y. Gao, X. He, Q. Huang, S. Chen, S. H. Kim and D. Wang, *Nat. Commun.*, 2017, **8**, 850.

11 J. Qian, W. A. Henderson, W. Xu, P. Bhattacharya, M. Engelhard, O. Borodin and J.-G. Zhang, *Nat. Commun.*, 2015, **6**, 6362.

12 S. Jiao, X. Ren, R. Cao, M. H. Engelhard, Y. Liu, D. Hu, D. Mei, J. Zheng, W. Zhao, Q. Li, N. Liu, B. D. Adams, C. Ma, J. Liu, J. G. Zhang and W. Xu, *Nat. Energy*, 2018, 1–8.

13 E. Cha, M. D. Patel, J. Park, J. Hwang, V. Prasad, K. Cho and W. Choi, *Nat. Nanotechnol.*, 2018, **13**, 337–343.

14 K. Liu, A. Pei, H. R. Lee, B. Kong, N. Liu, D. Lin, Y. Liu, C. Liu, P. chun Hsu, Z. Bao and Y. Cui, *J. Am. Chem. Soc.*, 2017, **139**, 4815–4820.

15 Y. Gao, Y. Zhao, Y. C. Li, Q. Huang, T. E. Mallouk and D. Wang, *J. Am. Chem. Soc.*, 2017, **139**, 15288–15291.

16 X. B. Cheng, R. Zhang, C. Z. Zhao, F. Wei, J. G. Zhang and Q. Zhang, *Adv. Sci.*, 2015, **3**, 1500213.

17 H. Liu, H. Zhou, B. S. Lee, X. Xing, M. Gonzalez and P. Liu, *ACS Appl. Mater. Interfaces*, 2017, **9**, 30635–30642.

18 H. Liu, X. Wang, H. Zhou, H.-D. Lim, X. Xing, Q. Yan, Y. S. Meng and P. Liu, *ACS Appl. Energy Mater.*, 2018, **1**, 1864–1869.

19 J. Wang, Y. Yamada, K. Sodeyama, E. Watanabe, K. Takada, Y. Tateyama and A. Yamada, *Nat. Energy*, 2018, **3**, 22–29.

20 S. Chen, J. Zheng, L. Yu, X. Ren, M. H. Engelhard, C. Niu, H. Lee, W. Xu, J. Xiao, J. Liu and J. G. Zhang, *Joule*, 2018, **2**, 1548–1558.

21 H. K. Reimschuessel and W. S. Creasy, *J. Polym. Sci.*, 1978, **16**, 845–860.

22 X. Wang, Y. Li and Y. S. Meng, *Joule*, 2018, **2**, 2225–2234.

23 N. D. Field and J. R. Schaefgen, *J. Polym. Sci.*, 1962, **58**, 533–543.

24 L. Ding, Y. Li, Y. Li, Y. Liang and J. Huang, *Eur. Polym. J.*, 2001, **37**, 2453–2459.

25 A. P. Krapcho, J. F. Weimaster, J. M. Eldridge, E. G. E. Jahngen, A. J. Lovey and W. P. Stephens, *J. Org. Chem.*, 1978, **43**, 138–147.

26 J. Lee and M. H. Litt, *Macromolecules*, 2000, **33**, 1618–1627.

27 Y. C. Jung, M. S. Park, D. H. Kim, M. Ue, A. Eftekhari and D. W. Kim, *Sci. Rep.*, 2017, **7**, 17482.

28 F. Wu, J. T. Lee, N. Nitta, H. Kim, O. Borodin and G. Yushin, *Adv. Mater.*, 2015, **27**, 101–108.

29 G. Bieker, M. Winter and P. Bieker, *Phys. Chem. Chem. Phys.*, 2015, **17**, 8670–8679.

30 H. Ota, K. Shima, M. Ue and J. Yamaki, *Electrochim. Acta*, 2004, **49**, 565–572.

31 Z. Hu, S. Zhang, S. Dong, Q. Li, G. Cui and L. Chen, *Chem. Mater.*, 2018, **30**, 4039–4047.

32 Q. Zhao, X. Liu, S. Stalin, K. Khan and L. A. Archer, *Nat. Energy*, 2019, **4**, 365.

33 S. Wei, Z. Cheng, P. Nath, M. D. Tikekar, G. Li and L. A. Archer, *Sci. Adv.*, 2018, **4**, eaao6243.

34 M. D. Tikekar, G. Li, L. A. Archer and D. L. Koch, *J. Electrochem. Soc.*, 2018, **165**, A3697–A3713.

35 X. Wang, M. Zhang, J. Alvarado, S. Wang, M. Sina, B. Lu, J. Bouwer, W. Xu, J. Xiao, J. G. Zhang, J. Liu and Y. S. Meng, *Nano Lett.*, 2017, **17**, 7606–7612.

36 Y. Li, Y. Li, A. Pei, K. Yan, Y. Sun, C. L. Wu, L. M. Joubert, R. Chin, A. L. Koh, Y. Yu, J. Perrino, B. Butz, S. Chu and Y. Cui, *Science (80-.).*, 2017, **358**, 506–510.

37 G. Wan, F. Guo, H. Li, Y. Cao, X. Ai, J. Qian, Y. Li and H. Yang, *ACS Appl. Mater. Interfaces*, 2018, **10**, 593–601.

38 I. A. Shkrob, J. F. Wishart and D. P. Abraham, *J. Phys. Chem. C*, 2015, **119**, 14954–14964.

39 X. Q. Zhang, X. B. Cheng, X. Chen, C. Yan and Q. Zhang, *Adv. Funct. Mater.*, 2017, **27**, 1605989.

40 S. Chen, J. Zheng, D. Mei, K. S. Han, M. H. Engelhard, W. Zhao, W. Xu, J. Liu and J. G. Zhang, *Adv. Mater.*, 2018, **30**, 1706102.

41 C. Yan, X. B. Cheng, Y. Tian, X. Chen, X. Q. Zhang, W. J. Li, J. Q. Huang and Q. Zhang, *Adv. Mater.*, 2018, **30**, 1707629.

42 X. Ren, Y. Zhang, M. H. Engelhard, Q. Li, J. G. Zhang and W. Xu, *ACS Energy Lett.*, 2018, **3**, 14–19.

43 L. Suo, W. Xue, M. Gobet, S. G. Greenbaum, C. Wang, Y.

View Article Online
DOI: 10.1039/C9TA02341K

Chen, W. Yang, Y. Li and J. Li, *Proc. Natl. Acad. Sci.*, 2018, **115**, 1156–1161.

44 K. Xu, *Chem. Rev.*, 2014, **114**, 11503–11618.

45 G. Li, Q. Huang, X. He, Y. Gao, D. Wang, S. H. Kim and D. Wang, *ACS Nano*, 2018, **12**, 1500–1507.

46 D. Lin, Y. Liu, W. Chen, G. Zhou, K. Liu, B. Dunn and Y. Cui, *Nano Lett.*, 2017, **17**, 3731–3737.

47 L. J. Krause, V. L. Chevrier, L. D. Jensen and T. Brandt, *J. Electrochem. Soc.*, 2017, **164**, A2527–A2533.

48 Y. Carmeli, M. Babai and H. Yamin, *J. Electrochem. Soc.*, 1994, **141**, 603–611.

49 D. Aurbach, B. Markovsky, A. Shechter, Y. Ein-Eli and H. Cohen, *J. Electrochem. Soc.*, 1996, **143**, 3809–3820.

View Article Online
DOI: 10.1039/C9TA02341K

In-situ formed poly(vinylene carbonate)-lithium iodide gel electrolyte enables stable cycling of lithium metal and a thermal shutdown function.